geosciences

MDPI

Article

Verification of a System for Sustainable Research on Earthquake-Induced Soil Liquefaction in 1-g Environments

Julijana Bojadjieva *, Vlatko Sheshov, Kemal Edip and Toni Kitanovski

Institute of Earthquake Engineering and Engineering Seismology-IZIIS, Ss. Cyril and Methodius University, 1000 Skopje, North Macedonia

* Correspondence: jule@iziis.ukim.edu.mk

Abstract: Within the presented research, model tests were performed in 1-g conditions to investigate the liquefaction potential of Skopje sand as a representative soil from the Vardar River's terraces in N. Macedonia. A series of shaking table tests were performed on a fully saturated, homogeneous model of Skopje sand in the newly designed and constructed laminar container in the Institute of Earthquake Engineering and Engineering Seismology (IZIIS), Skopje, N. Macedonia. The liquefaction depth in each shaking test was estimated based on the measured acceleration and pore water pressure as well as the frame movements of the laminar container. The surface settlement measurements indicated that the relative density increased by ~12% after each test. The observations from the tests confirmed that liquefaction was initiated along the depth at approximately the same time. The number of cycles required for liquefaction increased as the relative density increased. As the pore water pressure rose and reached the value of the effective stresses, the acceleration decreased, thus the period of the soil started to elongate. The results showed that the investigated Skopje sand was highly sensitive to void parameters and, under specific stress conditions, the liquefaction that occurred could be associated with large deformations. The presented experimental setup and soil material represent a well-proven example of a facility for continuous and sustainable research in earthquake geotechnical engineering.

Keywords: liquefaction; laminar container; shaking table test

Citation: Bojadjieva, J.; Sheshov, V.; Edip, K.; Kitanovski, T. Verification of a System for Sustainable Research on Earthquake-Induced Soil Liquefaction in 1-g Environments. *Geosciences* **2022**, *12*, 363. https://doi.org/10.3390/geosciences12100363

Academic Editors: Francesca Bozzoni, Claudia Meisina and Jesus Martinez-Frias

Received: 15 August 2022
Accepted: 22 September 2022
Published: 29 September 2022

1. Introduction

Over time, earthquakes have continued to provide lessons and data, and researchers and practitioners have become increasingly aware of additional potential problems associated with soils. In parallel, there has been an increasing fragility of our urban society toward natural disasters in general and earthquakes in particular. Experiences from recent earthquakes have demonstrated that a high percentage of damage and economic losses is related to geotechnical hazards and soil liquefaction [1]. The high losses incurred due to destructive earthquakes have given rise to the need for assessments and a better understanding of the soil behavior under cyclic loading.

Several cases of soil failure and liquefaction manifestation have been reported in Southern Europe, for example, Montenegro, 1979 [2], and more recently, during the Emilia earthquake sequence in Italy in 2012 [3–6], the Kraljevo earthquake in Serbia in 2013 [7], the Durres earthquake in Albania [8–10], and the latest 2020 Petrinje earthquake in Croatia [11,12].

Liquefaction is a specific type of failure mode, which may occur when cohesionless soils are exposed to cyclic loading in an undrained state. In this case, there is a probability that the effective stresses will reach zero due to pore pressure build-up, and the soil will behave as a liquid with no bearing capacity. The first time the effective stress reaches zero, the soil tries to dilate and negative pore pressure is generated, which leads to an increase in the effective stresses. As cyclic loading continues, this pattern is repeated and an increase in shear strains is observed [13–16].

It has been shown that several important parameters influence the liquefaction potential of soils. These are the state of saturation, relative density, earthquake magnitude and

ground motion characteristics, effective overburden pressure, and fine contents. These and other parameters have been investigated by various researchers. The dissipation of the developed pore pressure following liquefaction can cause significant hazards. Tokimatsu and Seed, 1987 [17] and several other authors such as [18–22] are among the researchers who have studied earthquake-induced settlements due to liquefaction in free-field conditions.

Model tests are an excellent tool for simulating a prototype's performance and are widely reported in the literature [23–36]. Model tests can be performed under gravitational earth fields (1-g environments) and higher gravitational fields (multi-g environments, for example, centrifuge tests). Both shaking table and centrifuge model tests have certain benefits and constraints. Tests of 1-g environments involve a well-controlled large amplitude, multi-axis input motions, and simpler measurements and are justified if the purpose of the test is to confirm a numerical model or to investigate basic failure mechanisms. In order to test a geotechnical model, the type of container, which sets the boundary conditions of the soil, is very important. The ideal container provides the seismic response of the soil model identical to that obtained in the case of the prototype.

Even though no liquefaction occurrence was officially reported during the 1963 Skopje earthquake with a magnitude of 6.1, a lot of structural damage was officially confirmed to have been associated with large site amplification effects in the Vardar Valley [37]. Considering that there was no official seismic code at that time, no seismic registration network, and not much knowledge of the geotechnical properties of the city, liquefaction might have happened but was not registered or assessed due to the extensive structural damage and disaster management activities after the earthquake. The above-mentioned case histories in the Balkan region promoted the need for increasing awareness of geotechnical hazards associated with cyclic loading. This requires improved experimental and numerical techniques for earthquake mitigation. Within the presented research, comprehensive experimental investigations consisting of shaking table tests on a homogeneous sand model in a laminar container were performed at the Institute for Earthquake Engineering and Engineering Seismology (IZIIS) in Skopje, Macedonia to investigate the liquefaction potential of Skopje sand, a representative soil from the Vardar River terraces in N. Macedonia. The original experimental setup consisted of a newly designed and constructed laminar container developed to provide a long-term facility for the research of liquefaction- and cyclic-induced geotechnical phenomena in the IZIIS. In this paper, the validation of the laminar box behavior is presented through the shaking table tests on fully saturated cohesionless soil. The sand that was used in the shaking table tests is representative of the alluvial deposits around the Vardar River [38,39] and is referred to as Skopje sand. The performed investigations are a good resource for further sustainable research using geotechnical model testing on shaking tables in Southern Europe.

2. Skopje Sand–Material for Testing

The tested material referred to as Skopje sand was taken from a site next to the terraces of the Vardar River, which streams through the capital city of Skopje and is the biggest river in N. Macedonia. Besides the assumption that this alluvial sand is likely to be associated with liquefaction potential and large deformations during an earthquake, the selection of this material for testing is also justified by the expanded possibility for continuous and sustainable experimental research [39].

The grain size distribution curve of the sand (ISO/TS 17892-4:2004) is presented in Figure 1 (left) compared to other standard sands reported in the literature and used for research on liquefaction phenomena. It can be observed that the Skopje sand is inside the boundaries given by Terzaghi, 1996 [40] and represents high susceptibility to liquefaction. The shape of the sand particles is subangular and homogeneous, as shown in Figure 1 (right). The silicate analysis indicated that of the components in the sand, the highest percentage was that of silica oxides and thus the sand could be categorized as a siliceous sand material. Table 1 presents the main physical properties of Skopje sand.

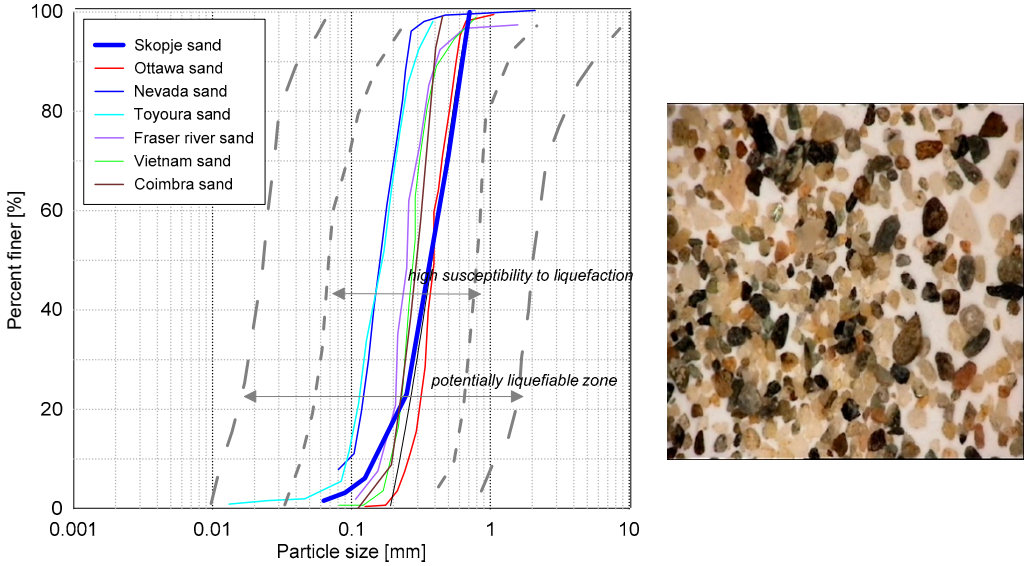

Figure 1. Grain size distribution compared with other sands from the literature (**left**) and particle shape of Skopje sand [zoom 40×] (**right**).

Table 1. Physical properties of Skopje sand.

e_{min} (Minimum Void Ratio)	e_{max} (Maximum Void Ratio)	Gs [kN/m^3] (Specific Gravity)	D_{50} [mm] (Median Particle Size Diameter)	Cu (Uniformity Coefficient)	Cc (Coefficient of Curvature)
0.95	0.51	2.615	0.26	1.8	0.8

3. Shaking Table Tests under 1-g Conditions

3.1. Description and Components of the Laminar Box

The soil container should simulate the propagation of the shear waves properly, producing a good presentation of the prototype behavior in a model test. The presence of inflexible and smooth end walls in a ground model introduces three unfavorable boundary effects, i.e., divergences in the deformations, stresses, and input excitations [26]. In order to apply flexibility to the walls of the container, a laminar system is introduced with shear stiffness limited to friction between the layers and the influence of a rubber membrane inside the container.

It is important to fulfill certain features of the laminar container such as confinement to the shaking table, flexibility, transparency, appropriate weight, etc. However, it is very difficult to fulfill all the essential features. For the last decade, many laminar boxes have been developed across the globe to better simulate prototype conditions such as that discussed in [41].

A laminar box is a container that allows the 'free' horizontal movement of a soil model and it is placed on a shaking table to simulate wave propagation through a soil layer of a finite thickness during earthquakes, [33]. The laminar box used for the experimental study presented in this paper (Figure 2) was designed by fulfilling the following conditions:

- The aluminum layers were designed to have minimal shear stiffness.
- The mass of the laminar box was much smaller compared to the mass of the soil.
- The membrane was designed to retain water and air, providing the possibility for saturated soil model testing.
- It allowed for the vertical settlement of the soil.
- Each aluminum layer had small dimensions for better shear movement together with the soil.

- The dimensions were large enough, providing the possibility for the improved simulation of the prototype.
- There was the possibility of increasing the confining pressure.
- The horizontal cross-section did not change during shaking.
- The shear stresses at the interface between the soil and the vertical wall were equal to the stresses in the horizontal plane.
- The free movement of soil along the transversal cross-section was enabled.
- Instrumentation setup and provision were easily managed.
- A stiff connection to the shaking table was enabled.

Figure 2. The constructed laminar box.

The three-dimensional layout of the designed container is shown in Figure 3. The container was built of the following main modules:

- Aluminum layers and ball bearings;
- A base plate with a saturation and drainage system in the floor;
- A steel frame, which was used to hold the laminar layers;
- An internal membrane providing saturation of the model and protecting the aluminum bearings from dust.

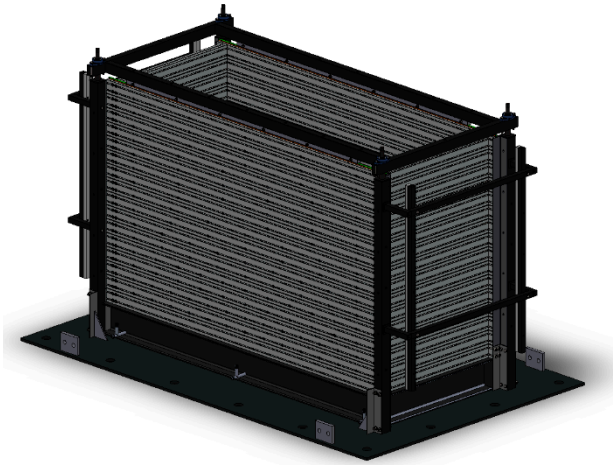

Figure 3. The 3D layout and main characteristics of the laminar container.

3.1.1. Aluminum Layers and Ball Bearings

Each aluminum layer represented a square ring of hollow profiles with a 40 × 80 mm^2 section. The whole container was composed of 16 layer rings. Transfer ball bearings were installed between the layers to provide two-dimensional motion in the horizontal plane, minimizing the friction between the layers. Transfer balls provided maximum sliding and minimum friction at the same time. In fact, the balls acted as a column connecting the lower and upper aluminum rings and preventing the surface from deformation. Rotating ball bearings were used between each ring where the gap between two adjacent layers was three mm, providing uniform distribution.

3.1.2. The Steel Frame

In order to assure the integrated stiffness of the laminar container, a steel frame, which provided an add-on for the shaking table, was used. On the top, static guides were installed in order to connect the top laminar layer. The steel frame was constructed in a way to allow for the easy setting of the transducers of the acquisition system. In order to provide fixation of the rings during the process of the installation of the sand, breaks were designed (Figure 4, left). When not fixed, the steel frame boundaries were covered with rubber, which provided dumping of the greater translational displacements of the laminar rings (Figure 4, right).

Figure 4. Laminar box with fixed laminar rings (**left**) and laminar box with free movement of the laminar rings (**right**).

3.1.3. Drainage System for Saturation

The bottom laminar layer was connected to U18 profiles, which were fixed to a steel base plate with dimensions of 2.7 × 1.7 × 0.015 m. The saturation of the soil model was assured with the design of double bottom plates, where the upper one was perforated enabling the water to pass below to the system of small pipes (Figure 5). The contact between the soil and the base plate of the container allowed good shear stress transition and, at the same time, saturation and drainage of the samples were enabled.

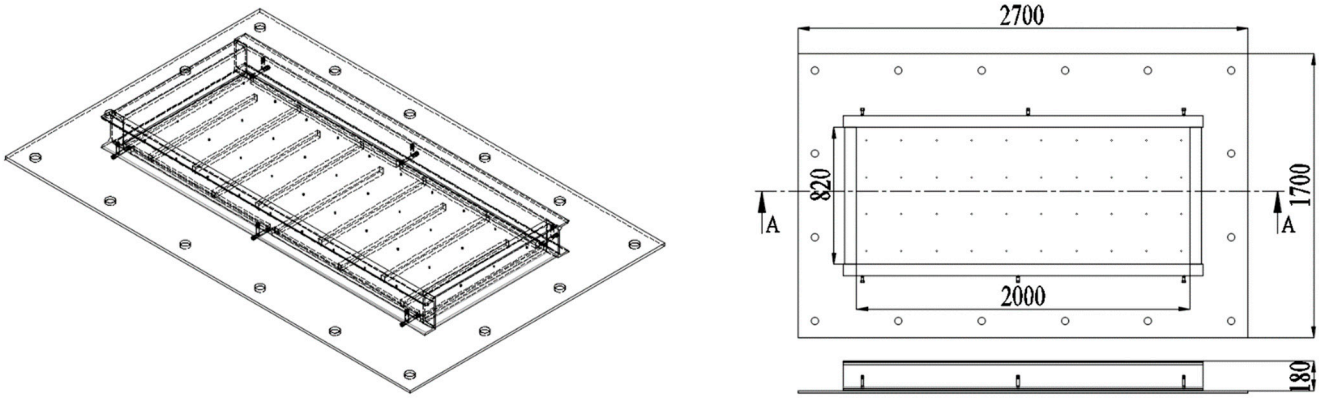

Figure 5. Base plate and saturation system.

The interior of the container was wrapped by a 1.2 mm-thick rubber membrane to assure a hydraulic cutoff system and the security of the ball bearings.

3.1.4. Method of Placement of the Soil

The method of placing the sand in the laminar box should fulfill the following criteria [42]: (1) it should be able to produce loose-to-dense sand beds in the unit weight range expected within an in situ soil deposit; (2) the sand bed must have a uniform void ratio throughout; (3) the samples should be well mixed without particle segregation, regardless of the particle gradation or fine contents; and (4) the sample preparation method should simulate the mode of soil deposition commonly found in the soil deposit being modeled.

Most widely spread are the dry pluviation/pouring devices, where dry sand is either "rained" over the surface of the model or poured close to the surface, creating a dry soil profile [43].

Dry pluviator devices can be split into three categories based on the area over which the sand is rained and the required number of axes of movement relative to the model: point pluviators, curtain pluviators, and carpet pluviators. With point pluviators, the sand exits from a relatively small opening, which is moved along three axes to cover the complete model area and maintain a constant falling height. Curtain pluviators are designed to pluviate a complete line of sand across the surface of the model and as such, they must be moved laterally across the model along one axis as well as vertically. Finally, carpet pluviators drop sand across the full surface area of the model, requiring only the vertical movement of the equipment. For the purpose of the so-called carpet pluviator technique for the installation of the sand in the laminar box, a sieve was constructed (Figure 6, left). Based on reported studies in the literature, the sieve was built of a wooden frame and perforated steel plate with holes of 10 mm (Figure 6, right). Calibration tests verified that the designed sieve was appropriate for the installation of the sand and that it provided uniform and homogenous layers of the soil.

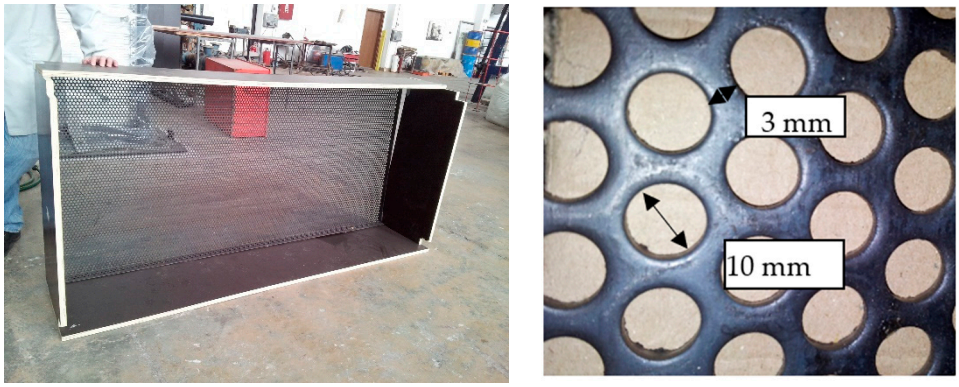

Figure 6. The constructed sieve for installing the sand.

3.1.5. Instrumentation

For the purpose of the model testing on the laminar box on the shaking table, the following measuring equipment transducers were used:

- Accelerometers–ACC;
- Linear variable displacement transducers–LVDT;
- Pore water pressure transducers–PWP;

The measuring of acceleration during the model testing was performed by accelerometers on the laminar rings, on the steel frame, and inside the sand. The used accelerometers had the following technical features:

Accelerometers placed on the laminar box (Figure 7):

- Sensor product name: Kistler 8712A5M1;
- Sensor Range Value: 5 g;
- Sensor Accuracy Value: 0.0004 g.

Accelerometers placed inside the sand:

- Sensor product name: PCB 333B50;
- Sensor Range Value: 49 m/s^2;
- Sensor Accuracy Value: 0.0005 m/s^2.

Figure 7. Accelerometer placed on the laminar ring.

Three important aspects had to be considered regarding the placed accelerometers inside the sand model [31]. First, they had to be stable, without the possibility of tilting

during the shaking. For that purpose, the accelerometers were placed on a previously made plastic support with dimensions of 5 cm × 5 cm × 2.5 cm (Figure 8). The larger area of the support provided a representation of a larger area of the soil model and also reduced the risk of tilting during the shaking. The lightweight mass of the support, the larger stiffness of the support, and the accelerometer provided the second aspect involving a better interaction between the accelerometer and the soil without any possibility for relative movement between them. The third important aspect was the working range of the frequencies of the transducers, which needed to be much higher than the frequency of the input motion of the shaking.

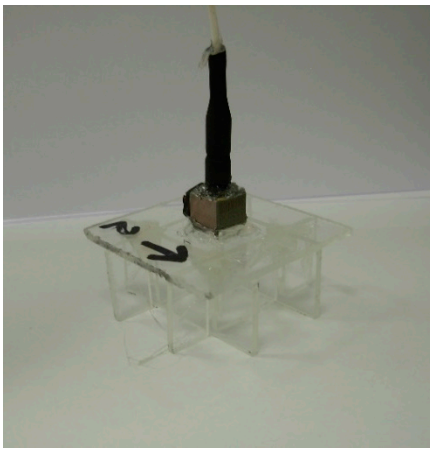

Figure 8. Accelerometer that is pressed into the soil.

Linear variable displacement transducers—LVDTs

To measure the horizontal displacements of the laminar rings and the soil, four LVDTs were used. They were placed on previously placed steel holders on the steel frame of the laminar rings, as presented in Figure 9. The used LVDTs had the following characteristics:

- Sensor product name: Macro Sensors DC 750-3000;
- Sensor Range Value: 76 mm;
- Sensor Accuracy Value: null.

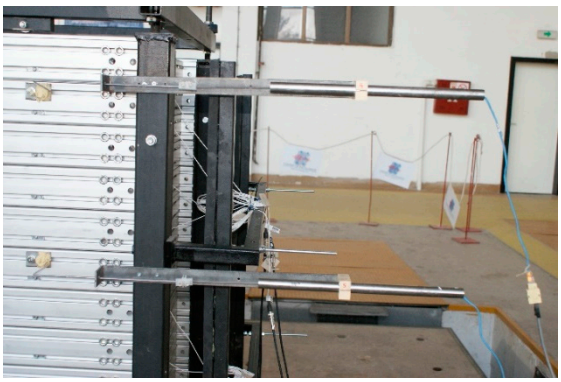

Figure 9. LVDTs placed on the steel frame of the laminar box.

Pore water pressure transducers–PWP (Figure 10)

Figure 10. PWP transducer (**left**) and PWP line prepared for the sand model (**right**).

To measure the excess pore water pressure in sand 6, six PWP transducers with the following characteristics were used:

- Sensor product name: Kyowa BPR-A-50KPS;
- Rated capacity 50 kPa;
- Weight 35 gr.

It is important to note that before using the PWP transducers, fully saturated conditions must be achieved in order to provide continuous and accurate measurements.

The PWP transducers were prepared previously and stacked on a string with a defined distance of 20 cm between them. In order to hold the "transducer line" straight during the installation of the sand (as shown in Figure 10), on the cable of the connected transducers at the end of the string, a small object of a proper weight was attached.

All the transducers described above were connected to the acquisition system from where the data were transferred to the computer.

3.2. Results of the Shaking Table Tests

A series of harmonic shaking table tests were carried out on a homogenous sand model in the laminar box. The main purpose of the performed tests was to simulate liquefaction initiation by observing physical measurements such as accelerations, displacements, and pore pressure development inside the sand and validate the design concepts of the laminar box (Table 2). The instrumentation setup is presented in Figure 11. The design concept of the laminar box was confirmed by a series of tests on the empty container, which is presented in more detail in Bojadjieva (2015) [39].

Table 2. Shaking table tests with harmonic excitation.

Test Name	Type	Frequency	Amplitude	Duration
Test_01	Harmonic	2 Hz	0.05 g	12 sec
Test_02	Harmonic	2 Hz	0.1 g	12 sec
Test_03	Harmonic	2 Hz	0.2 g	12 sec

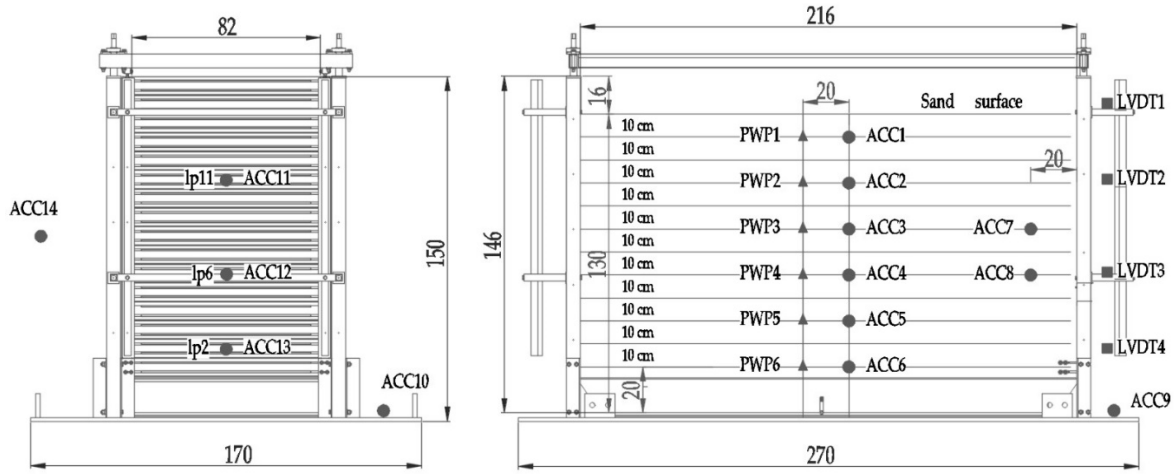

Figure 11. Instrumentation setup of the laminar box.

The initial relative density of the soil sample in the laminar box was determined as Dr = 38%. Figure 12 presents the soil model after installation of the sand and the amount of soil built in the 12 layers for better control of the achieved density. The sand was rained into already filled water layers in the laminar box in order to provide a fully saturated soil model.

Soil layer	Depth of soil layer [m]	Amount of soil [kg]
1	0.2	400
2	0.1	200
3	0.1	300
4	0.1	300
5	0.1	150
6	0.1	300
7	0.1	300
8	0.1	300
9	0.1	200
10	0.1	200
11	0.1	200
12	0.1	200
sum	1.3	3050

Figure 12. The sand model in the laminar box before testing (**left**) and amount of soil installed in the soil model (**right**).

The shaking table in the IZIIS had the following characteristics:

- Size: 5.0 m × 5.0 m
- Mass: 330 kN
- Maximum model mass: 400 kN with a height of 6.0 m
- Frequency range: 0–80 Hz
- Maximum horizontal acceleration: 0.70 g

The stiff connection of the laminar container to the shaking table was confirmed by the matching of the acceleration time history measured by the transducer at the base plate with the assigned input acceleration time history. The soil and the laminar box vibrated simultaneously, which was confirmed by the comparison of the acceleration recordings on the frame and the soil (Figure 13). From these graphs, the exact time of the initiation of liquefaction can be observed. From the start of the test up to the liquefaction manifestation, the acceleration values of the laminar container and the sand fit thoroughly. Following the liquefaction occurrence, the period of vibration became longer and the acceleration values decreased and tended to zero.

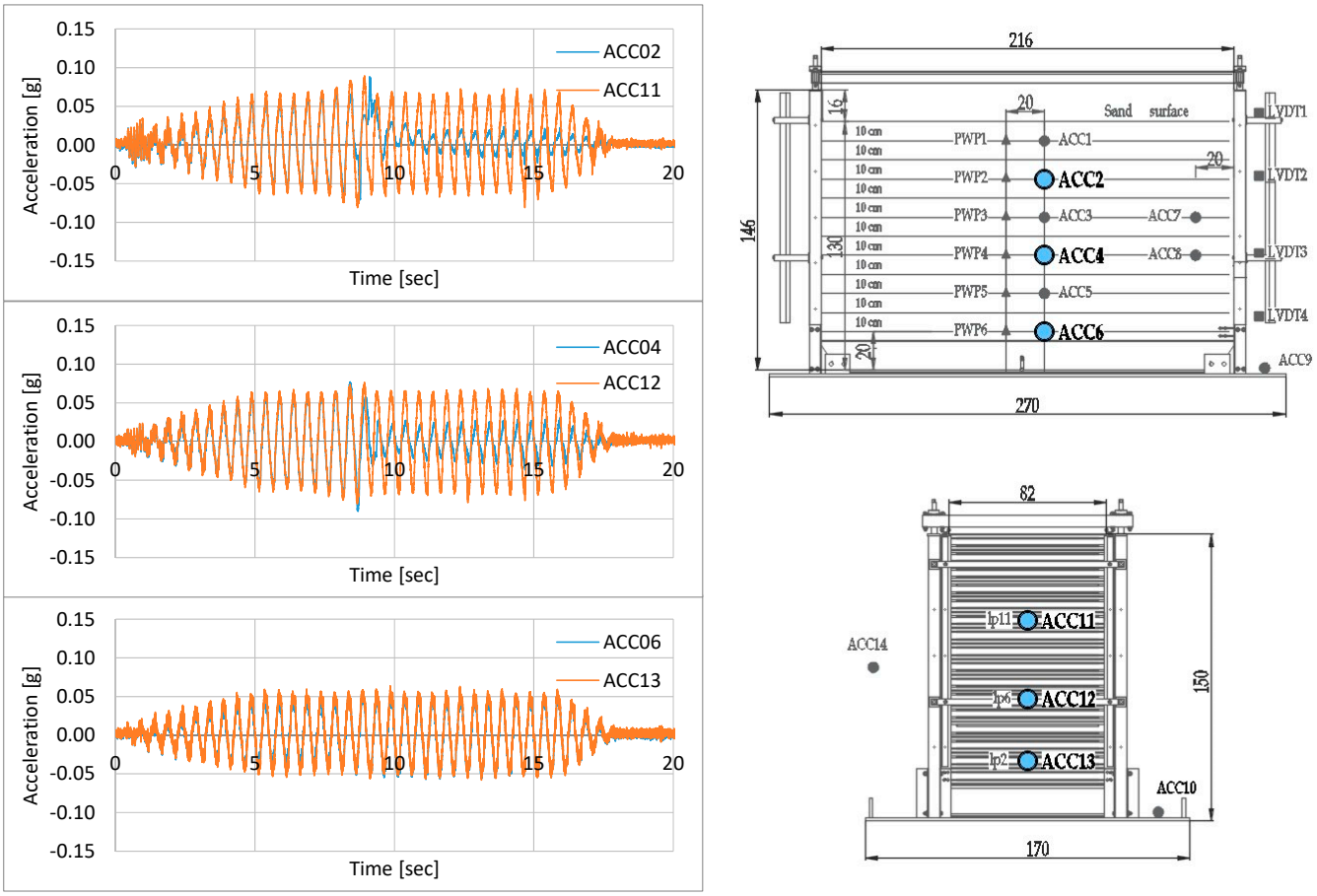

Figure 13. Acceleration time history on soil model and frame for test no. 1, 0.05 g (**left**) and position of the accelerometers on the instrumentation scheme (**right**).

Figure 14 presents the acceleration measurements in the middle of the sand layer ACC04 compared to the acceleration close to the laminar box boundaries ACC08 at a depth of −70 cm for test No. 1 (0.05 g). From the graph, it can be seen that the response of the soil matches the response of the container until the occurrence of liquefaction. Based on this observation, the shear beam type of the behavior of the laminar box can be validated by properly simulating the free-field conditions.

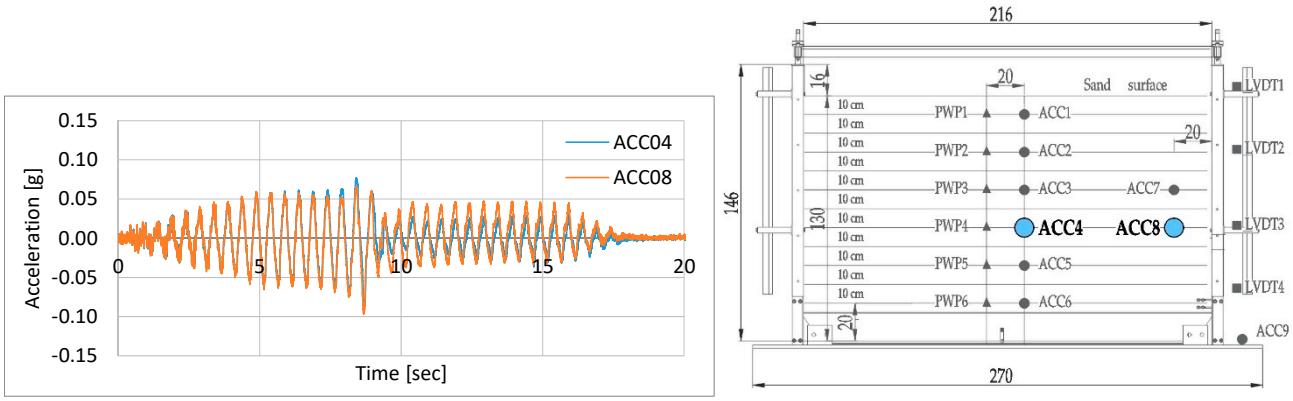

Figure 14. Acceleration time history measured on the sand model in the middle and near the boundaries (0.05 g) (**left**) and position of the accelerometers on the instrumentation scheme (**right**).

The observations from the performed three tests confirmed that liquefaction was initiated along the depth at approximately the same time. The number of cycles required

for liquefaction increased as the relative density increased. As the pore water pressure increased and reached the value of the effective stresses, the acceleration decreased, leading to the initiation of the soil period elongation. Figures 15–17 present the acceleration and pore water pressure time history measurements for each test consequently. The visible manifestation of the liquefaction initiation was observed during the tests characterized by sand boils (Figure 18).

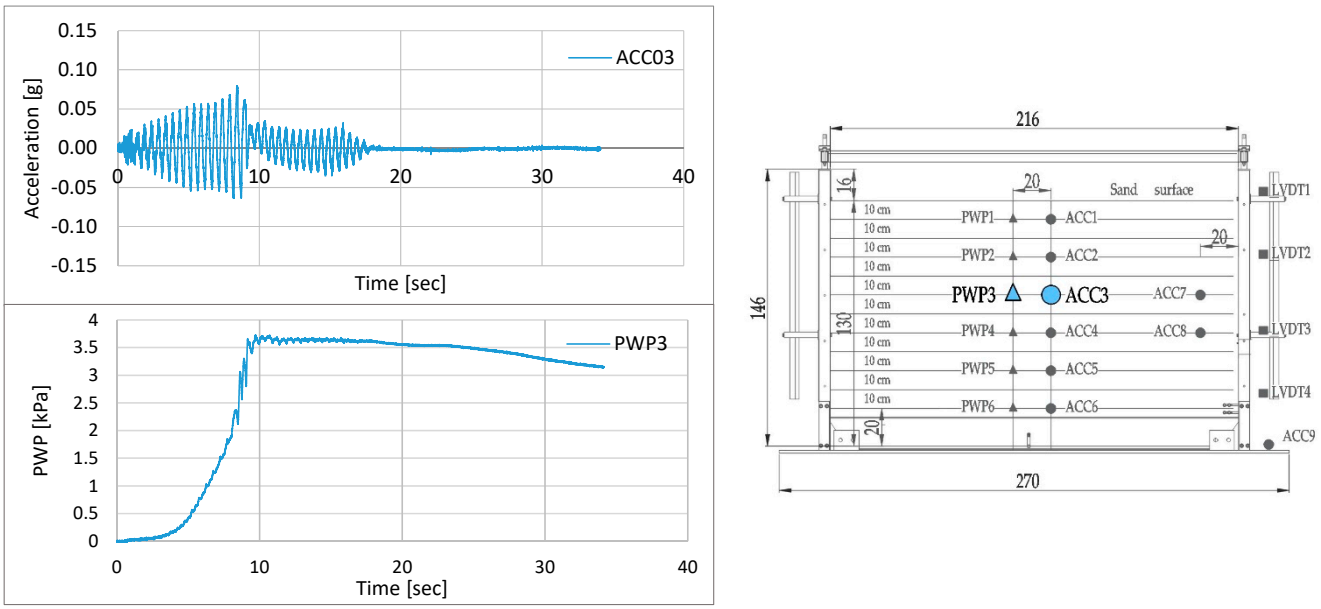

Figure 15. Liquefaction initiation—Acceleration and excess PWP measurements of the sand model at depth—50 cm (test no. 1, 0.05 g) (**left**) and position of the accelerometers and PWP transducers on the instrumentation scheme (**right**).

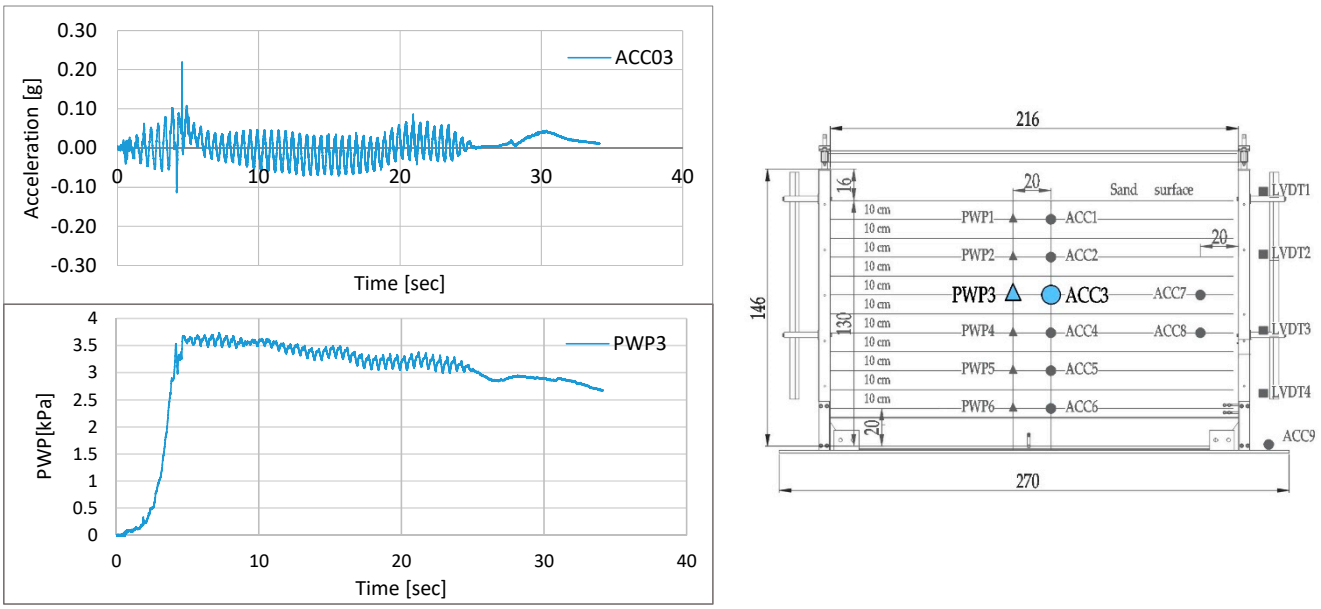

Figure 16. Liquefaction initiation—Acceleration and excess PWP measurements of the sand model at depth—50 cm (test no. 2, 0.1 g) (**left**), and position of the accelerometers and PWP transducers on the instrumentation scheme (**right**).

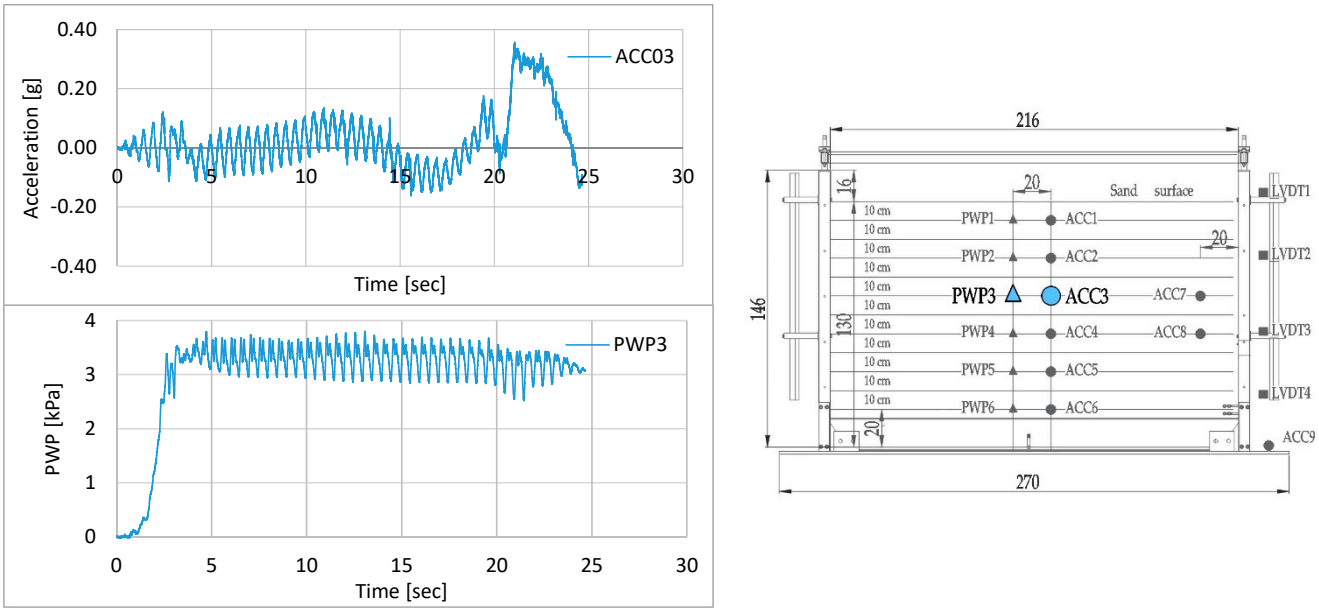

Figure 17. Liquefaction initiation—Acceleration and excess PWP measurements of the sand model at depth—50 cm (test no. 3, 0.2 g) (**left**) and position of the accelerometers and PWP transducers on the instrumentation scheme (**right**).

Figure 18. Visible manifestation of sand boils after liquefaction initiation (test No. 1).

Before the application of each shaking test, the extent of the densification was estimated manually, measuring the level of the soil surface at several points with respect to a referent point. In Table 3, the relative density after each test is given. The average relative density increased from 32 to 41% after the first shaking test, 53% after the second shaking test, and 65% after the third shaking test. It was observed that the relative density was increased by ~12% after each test.

Table 3. Measured settlements and densification after shaking.

Measuring Point	Settlement after Test No. 1 (0.05 g) [cm]	Settlement after Test No. 2 (0.1 g)	Settlement after Test No. 3 (0.2 g)
1	3.2	2.8	4.9
2	3.7	2.8	4.3
3	2.8	4.3	4.0
4	1.4	3.8	4.2
5	2.8	3.7	3.5
6	1.6	4.4	3.8
7	3.8	3.6	3.3
8	3.3	3.5	3.5
9	3.6	3.8	3.0
Average settlements per test [cm]	2.9	3.6	3.8
Relative density Dr (%)	41%	53%	65%

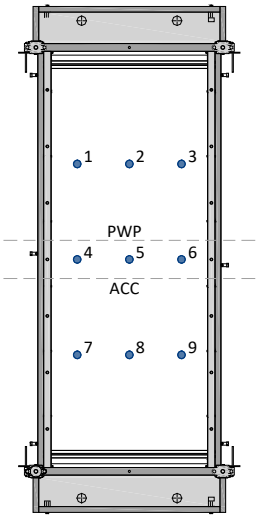

Following each shaking test, the generated excess pore pressure was allowed to dissipate for approximately 45 min to one hour.

4. Conclusions

A 1-g model testing system was used to test liquefaction in saturated sands through one-dimensional shaking table tests. A series of shaking table tests were performed on a homogenous sand model installed in a laminar box in the IZIIS at full scale. Skopje sand material was used for the shaking table tests. The system was composed of a laminar box, a sand model, a sieve for installation of the sand, a water supply system, instrumentation, and related testing hardware. The performed investigations were mainly aimed at:

- The validation of the design concepts of the laminar box.
- Simulations of the liquefaction phenomena based on the physical measurements of accelerations, displacements, and pore pressure transducers inside the geo-model.
- Based on these test results, the following can be summarized:
- The designed laminar box was tested to see whether it could be used to investigate the liquefaction phenomena and cyclic responses of cohesionless soils. The laminar box exhibited excellent behavior, and the results confirmed that the design criteria were fulfilled and that the laminar box could be used in further model tests of geo-models. The results showed that the response of the soil was essentially that of a shear beam simulating free-field conditions and that the effectiveness of the laminar box system for the shaking table tests was satisfactory for dynamic model tests under the conditions of 1-g gravity. The sand that was used in the shaking table tests was representative of the alluvial deposits around the Vardar River and the performed investigations could provide a good basis for further definitions and raising awareness about the liquefaction hazards in the Republic of North Macedonia. We strongly believe that this new design for a laminar container will overcome many of the shortcomings of previous types of laminar boxes or shear boxes related to boundary conditions, saturation of sand, etc.
- The soil sample was prepared by the so-called carpet pluviator method through a sieve that was designed based on the capacities of the laboratory. The uniformity and

the density of the soil specimen prepared inside the box using this method were found to be satisfactory for loose sand deposits that are prone to liquefaction.

- The manifestation of the liquefaction was observed through acceleration and pore water pressure time response of the soil model and the frame of the laminar container. Sand liquefaction occurred within a certain depth instead of the whole specimen. The liquefaction depth in each shaking test was estimated based on the measured pore water pressure and frame movements. The surface settlement was manually measured at several points and the relative density after each shaking test was defined. It was observed that the relative density increased by ~12% after each test.
- The observations from the performed three tests confirmed that liquefaction was initiated along the depth at approximately the same time.
- The number of cycles required to initiate liquefaction increased as the relative density increased.
- The time history of the generation of pore water pressure was measured. Following the liquefaction occurrence, the period of vibration became longer, and the acceleration values decreased and tended to zero.
- The presented experimental setup and soil material represent a well-proven example of a facility for continuous and sustainable research in earthquake geotechnical engineering. The results have shown that the investigated Skopje sand is very sensitive to void parameters and that, under specific stress conditions, liquefaction associated with large deformations may occur.

Author Contributions: Conceptualization, J.B. and V.S.; methodology, J.B., V.S. and K.E.; validation, J.B., V.S. and K.E.; formal analysis, J.B.; investigation, J.B., V.S., K.E. and T.K.; writing—original draft preparation, J.B.; writing—review and editing, J.B., V.S. and K.E.; visualization, J.B.; supervision, V.S.; project administration, V.S.; funding acquisition, V.S. All authors have read and agreed to the published version of the manuscript.

Funding: The research and design were supported by the European FP7 Project UREDITEME REGPOT-2008-1 (Upgrading of research equipment for dynamic testing of large-scale models), grant no. 230099, https://cordis.europa.eu/project/id/230099 (accessed on 22 May 2022).

Institutional Review Board Statement: Not applicable.

Informed Consent Statement: Not applicable.

Conflicts of Interest: The authors declare no conflict of interest.

References

1. Cubrinovski, M.; Green, R.; Allen, J.; Ashford, S.; Bowman, E.; Bradley, B.; Cox, B.; Hutchinson, T.; Kavazanjian, E.; Orense, R.; et al. *Geotechnical Reconnaissance of the 2010 Darfield (New Zealand) Earthquake*; University of Canterbury: Christchurch, New Zealand, 2010.
2. Talaganov, K.; Petrovski, J.; Mihailov, V. Soil Liquefaction Seismic Risk Analysis Based on Post 1979 Earthquake Observations in Montenegro. In Proceedings of the First International Conference on Recent Advances in Geotechnical Earthquake Engineering & Soil Dynamics, Missouri University of Science and Technology, St. Louis, MO, USA, 26 April–3 May 1981.
3. Alessio, G.; Alfonsi, L.; Brunori, C.A.; Burrato, P.; Casula, G.; Cinti, F.R.; Civico, R.; Colini, L.; Cucci, L.; De Martini, P.M. Liquefaction Phenomena Associated with the Emilia Earthquake Sequence of May–June 2012 (Northern Italy). *Nat. Hazards Earth Syst. Sci.* **2013**, *13*, 935–947.
4. Fioravante, V.; Giretti, D.; Abate, G.; Aversa, S.; Boldini, D.; Capilleri, P.P.; Cavallaro, A.; Chamlagain, D.; Crespellani, T.; Dezi, F.; et al. Earthquake Geotechnical Engineering Aspects: The 2012 Emilia-Romagna Earthquake (Italy). In Proceedings of the Seventh International Conference on Case Histories in Geotechnical Engineering, Lecture No. EQ-5. Chicago, IL, USA, 29 April–4 May 2013.
5. Di Ludovico, M.; Chiaradonna, A.; Bilotta, E.; Flora, A.; Prota, A. Empirical Damage and Liquefaction Fragility Curves from 2012 Emilia Earthquake Data. *Earthq. Spectra* **2020**, *36*, 507–536. [CrossRef]
6. Lai, C.G.; Bozzoni, F.; Mangriotis, M.D.; Martinelli, M. Soil liquefaction during the May 20, 2012 M5.9 Emilia earthquake, Northern Italy: Field reconnaissance and post-event assessment. *Earthq. Spectra* **2015**, *31*, 2351–2373. [CrossRef]
7. Antonijevic, S.K.; Arroucau, P.; Vlahovic, G. Seismotectonic Model of the Kraljevo 3 November 2010 M w 5.4 Earthquake Sequence. *Seismol. Res. Lett.* **2013**, *84*, 600–610. [CrossRef]

8. Sextos, A.; Stefanidou, S.; Baltzopoulos, G.; Fragiadakis, M.; Giarlelis, C.; Lombardi, L.; Markogiannaki, O.; Mavroulis, S.; Plaka, A.; Pnevmatikos, N.; et al. ETAM Report on the Albania Earthquake of November 26, 2019. Structural and Geotechnical Damage. 2020. Available online: https://www.researchgate.net/publication/346008855_ETAM_Report_on_the_Albania_earthquake_of_November_26_2019_Structural_and_Geotechnical_Damage?channel=doi&linkId=5fb574e24585154a5fec766d&showFulltext=true (accessed on 22 May 2022).
9. Fischer, E.; Hakhamaneshi, M.; Alam, M.; Alberto, Y.; Aranha, C.; Diaz-Fanas, G.; Wilfrid, D.; Gartner, M.; Hassan, W.; Isufi, B.; et al. EERI VERT Albania Earthquake Phase 1 Report; DesignSafe-CI. 2019. Available online: https://www.designsafe-ci.org/data/browser/public/designsafe.storage.published/PRJ-2649 (accessed on 22 May 2022).
10. Mavroulis, S.; Lekkas, E.; Carydis, P. Liquefaction Phenomena Induced by the 26 November 2019, Mw= 6.4 Durrës (Albania) Earthquake and Liquefaction Susceptibility Assessment in the Affected Area. *Geosciences* **2021**, *11*, 215. [CrossRef]
11. Amoroso, S.; Barbača, J.; Belić, N.; Kordić, B.; Brčić, V.; Budić, M.; Civico, R.; De Martini, P.M.; Hećej, N.; Kurečić, T.; et al. Liquefaction Field Reconnaissance Following the 29th December 2020 Mw 6.4 Petrinja Earthquake (Croatia). In *EGU General Assembly Conference Abstracts*; EGU: Munich, Germany, 2021; p. EGU21-16584.
12. Baize, S.; Amoroso, S.; Belić, N.; Benedetti, L.; Boncio, P.; Budić, M.; Cinti, F.R.; Henriquet, M.; Jamšek Rupnik, P.; Kordić, B.; et al. Environmental Effects and Seismogenic Source Characterization of the December 2020 Earthquake Sequence near Petrinja, Croatia. *Geophys. J. Int.* **2022**, *230*, 1394–1418. [CrossRef]
13. Kramer, S.L. *Geotechnical Earthquake Engineering*; Pearson Education India: Noida, India, 1996.
14. Chen, Y.M.; Liu, H.L.; Zhou, Y.D. Analysis on Flow Characteristics of Liquefied and Post-liquefied Sand. *Chin. J. Geotech. Eng.* **2006**, *28*, 1139–1143.
15. Chen, G.; Zhou, E.; Wang, Z.; Wang, B.; Li, X. Experimental Study on Fluid Characteristics of Medium Dense Saturated Fine Sand in Pre- and Post-liquefaction. *Bull. Earthq. Eng.* **2016**, *14*, 2185–2212.
16. Flora, A.; Chiaradonna, A.; Bilotta, E.; Fasano, G.; Mele, L.; Lirer, S.; Pingue, L.; Fanti, F. Field Tests to Assess the Effectiveness of Ground Improvement for Liquefaction Mitigation. In *Earthquake Geotechnical Engineering for Protection and Development of Environment and Constructions*; CRC Press: Boca Raton, FL, USA, 2019; pp. 740–752.
17. Tokimatsu, K.; Seed, H.B. Evaluation of Settlements in Sands due to Earthquake Shaking. *J. Geotech. Eng.* **1987**, *113*, 861–878. [CrossRef]
18. Ishihara, K.; Yoshimine, M. Evaluation of Settlements in Sand Deposits Following Liquefaction During Earthquakes. *Soils Found.* **1992**, *32*, 173–188. [CrossRef]
19. Franke, K.W.; Peterson, B.D.; Error, B.M.; He, J.; Harper, J.N. Probabilistic Seismic Loading Considerations for the Assessment of Liquefaction-Induced Volumetric Settlements in the Free Field. *J. Geotech. Geoenviron. Eng.* **2021**, *147*, 04020175. [CrossRef]
20. Geyin, M.; Maurer, B.W. An Analysis of Liquefaction-induced Free-field Ground Settlement Using 1,000+ Case Histories: Observations vs. State-of-Practice Predictions. In *Geo-Congress 2019: Earthquake Engineering and Soil Dynamics 2019, March*; American Society of Civil Engineers: Reston, VA, USA, 2019; pp. 489–498.
21. Lirer, S.; Mele, L. On the Apparent Viscosity of Granular Soils During Liquefaction Tests. *Bull. Earthq. Eng.* **2019**, *17*, 5809–5824. [CrossRef]
22. Mele, L. An Experimental Study on the Apparent Viscosity of Sandy Soils: From Liquefaction Triggering to Pseudo-plastic Behaviour of Liquefied Sands. *Acta Geotech.* **2022**, *17*, 463–481. [CrossRef]
23. Prasad, S.K.; Towhata, I.; Chandradhara, G.P.; Nanjundaswamy, P. Shaking Table Tests in Earthquake Geotechnical Engineering. *Curr. Sci.* **2004**, *87*, 1398–1404.
24. Ueng, T.S. Shaking Table Tests for Studies of Soil Liquefaction and Soil-Pile Interaction. *Geotech. Eng.* **2010**, *41*, 29.
25. Kokusho, T. Current State of Research on Flow Failure Considering Void Redistribution in Liquefied Deposits. *Soil Dyn. Earthq. Eng.* **2003**, *23*, 585–603. [CrossRef]
26. Carvalho, A.T.; Bilé Serra, J.; Oliveira, F.; Morais, P.; Ribeiro, A.R.; Santos Pereira, C. Design of Experimental Setup for 1 g Seismic Load Tests on Anchored Retaining Walls. In *Physical Modelling in Geotechnics*; Springman, S., Laue, J., Seward, L., Eds.; Taylor & Francis Group: London, UK, 2010; ISBN 978–0-415–59288–8.
27. Coelho, P. In situ Densification as a Liquefaction Resistance Measure for Bridge Foundations. Ph.D. Thesis, Churchill College, Cambridge, UK, 2007.
28. Cubrinovski, M.; Kokusho, T.; Ishihara, K. Interpretation from Large-Scale Shake Table Tests on Piles Undergoing Lateral Spreading in Liquefied Soils. *Soil Dyn. Earthq. Eng.* **2006**, *26*, 275–286. [CrossRef]
29. Taylor, C.A.; Dar, A.R.; Crew, A.J. Shaking Table Modelling of Seismic Geotechnical Problems. In Proceedings of the 10th European Conference on Earthquake Engineering, Vienna, Austria, 28 August–2 September 1994; Volume 4, pp. 441–446.
30. Orense, R.P.; Morimoto, I.; Yamamoto, Y.A.; Yumiyama, T.; Yamamoto, H.; Sugawara, K. Study on Wall-type Gravel Drains as Liquefaction Countermeasure for Underground Structures. *Soil Dyn. Earthq. Eng.* **2003**, *23*, 19–39. [CrossRef]
31. Sesov, V. Dynamic Behavior of Potentially Nonstable Layers and Application of a Model for Decreasing the Seismic Risk of Liquefaction Occurrence. Ph.D. Thesis, University Ss. Cyril and Methodius, Institute of Earthquake Engineering and Engineering Seismology-IZIIS, Skopje, Macedonia, 2003.
32. Towhata, I. Development of Geotechnical Earthquake Engineering in Japan. *6th Int. Conf. Soil Mech. Geotech. Eng. Osaka Japan* **2004**, *1*, 251–291.

33. Jafarzadeh, F. Design and Evaluation Concepts of Laminar Shear Box for 1g Shaking Table Tests. In Proceedings of the 13th World Conference on Earthquake Engineering, No. 1391. Vancouver, BC, Canada, 1–6 August 2004.
34. Arulmoli, K.; Muraleetharan, K.K.; Hossain, M.M.; Fruth, L.S. *VELACS: Verification of liquefaction. Analyses by centrifuge studies, laboratory testing program*; Report no. 90-0562; The Earth Technology Corporation: Irvine, CA, USA, 1992.
35. El Ghoraiby, M.A.; Park, H.; Manzari, M. LEAP-2017 GWU Laboratory Tests. DesignSafe-CI, Dataset. 2018. Available online: https://www.designsafe-ci.org/data/browser/public/designsafe.storage.published/PRJ-1783 (accessed on 22 May 2022).
36. Özcebe, A.G.; Giretti, D.; Bozzoni, F.; Fioravante, V.; Lai, C.G. Centrifuge and numerical modelling of earthquake-induced soil liquefaction under free-field conditions and by considering soil–structure interaction. *Bull. Earthq. Eng.* **2021**, *19*, 47–75. [CrossRef]
37. Poceski, A. The Ground Effects of the Skopje July 26, 1963 Earthquake. *Bull. Seismol. Soc. Am.* **1969**, *59*, 1–22. [CrossRef]
38. Bojadjieva, J.; Sesov, V.; Edip, K. Sand Characterization for Experimental Studies on Liquefaction Phenomena. In Proceedings of the GE Conference, from Case History to Practice in Honour of Prof. Kenji Ishihara, Istanbul, Turkey, 17–19 June 2013.
39. Bojadjieva, J. Dynamic Behavior of Saturated Cohesionless Soils Based on Element And 1-G Experiments. Ph.D. Thesis, Ss. Cyril and Methodius: Institute of Earthquake Engineering and Engineering Seismology, Skopje, Macedonia, 2015.
40. Terzaghi, K.; Peck, R.B.; Mesri, G. *Soil Mechanics in Engineering Practice*; John Wiley & Sons: Hoboken, NJ, USA, 1996.
41. Turan, A.; Hinchberger, S.D.; El Naggar, H. Design and Commissioning of a Laminar Soil Container for Use on Small Shaking Tables. *Soil Dyn. Earthq. Eng.* **2009**, *29*, 404–414. [CrossRef]
42. Gade, V.K.; Dave, T.N.; Chauhan, V.B.; Dasaka, S.M. Portable Traveling Pluviator to Reconstitute Specimens of Cohesionless Soils. In *Proceedings of the Indian Geotechnical Conference Roorkee*; University in Roorkee: Roorkee, India, 2013.
43. Stringer, M.E.; Pedersen, L.; Nuss, B.D.; Wilson, D.W. Design and Use of a Rotating Spiral Pluviator for Creating Large Sand Models. In *ICPMG2014 Physical Modelling in Geotechnics*; CRC Press: Boca Raton, FL, USA, 2013; pp. 253–258.